

A numerical solution based parameter estimation method for flash thermal diffusivity measurements

Liguo Chen ^{a,*}, David R. Clarke ^{a,b,1}

^a Mechanical Engineering Department, University of California, Santa Barbara, CA 93106, United States

^b Materials Department, University of California, Santa Barbara, CA 93106, United States

ARTICLE INFO

Article history:

Received 29 August 2008

Accepted 2 October 2008

Available online 25 November 2008

PACS:

66.30.Xj

Keywords:

Thermal flash

Diffusivity

Parameter estimation

Heat loss

Finite pulse

ABSTRACT

A data reduction method based on numerical solutions of the heat conduction equation has been developed for obtaining thermal diffusivity values from thermal flash measurements. Using the new method, the computed evolution in temperature is fitted to the measured temperature evolution instead of using the $t_{1/2}$ point alone, as is done in many other analyzes. The numerical solutions used are based on the finite-difference technique applied to the heat conduction equation including all the boundary conditions. A nonlinear least-squares regression technique is used to estimate simultaneously the thermal diffusivity, the heat transfer coefficient and the absorbed energy. Also, the effect of a finite pulse-width can be corrected without knowing the exact shape of the heat pulse.

Published by Elsevier B.V.

1. Introduction

Since its introduction in 1961 [1], the thermal flash technique has become a standard testing method for measuring the thermal diffusivity of solids. In the test, a thin disk specimen is subjected to a high-intensity, short duration radiant energy pulse. The energy of the pulse is absorbed on the front surface of the specimen and the thermal diffusivity value is computed from the resulting temperature response on the back surface of the sample, typically measured by an infrared (IR) detector. The variation in back surface temperature with time following the thermal pulse is referred to as a “Thermogram”. The model presented by Parker et al. [1] assumes uniform heating of the front surface, no heat losses, and an infinitesimally short pulse duration. In an actual measurement, nearly every one of these assumptions is violated to some extent. Consequently the analysis technique had been refined several times to account for various assumptions [2–8].

By using the least square curve fitting data reduction methods [10–13,15], the quality of experimental data can be checked by observing deviations between the experimental data and the theoretical curve. For instance, poor quality data resulting from nonuni-

form heating, drift of the specimen temperature, or slow response of the temperature-detection system, can be identified quickly. Thus, only good quality experimental data are selected, and therefore, thermal diffusivity values with smaller experimental uncertainty are obtained. This parameter estimation approach has become a common technique in this area.

Up until now analytical solutions have mostly been used in this parameter estimation approach, but become more and more expensive to implement because of the increasing complexity. In some cases, there is no analytical solution. In our method, we use a numerical solution approach instead. It has the advantage that nearly all boundary conditions, which can have an influence on the measurement, can be taken into account in a straightforward manner. For simple boundary conditions the calculation time for the numerical solution can exceed the time needed for the evaluation of the analytical solution, but for more complex conditions, the increasing computing speed and memory makes a numerical solution more viable. As far as we know, this numerical solution approach has never been used in this area yet.

In this paper, we will explain how this numerical solution approach used in the parameter estimation method. The thermal diffusivity of the sample and the heat transfer coefficient as well as the absorbed energy can be estimated simultaneously. Also by adapting the method of Azumi and Takahashi [25], the finite pulse-width effect can also be corrected without knowing the exact pulse shape of the flash source. Precautions on picking the data

* Corresponding author. Tel.: +1 805 304 6557.

E-mail addresses: lgchen@engr.ucsb.edu (L. Chen), clarke@engineering.ucsb.edu (D.R. Clarke).

¹ Tel.: +1 805 893 8275.

fitting range using this method are pointed out. The accuracy of this method was first checked by applying it on sets of numerical generated data. Then the results on real experimental data are compared with the other traditional methods.

2. Theoretical models

The formulae needed for the data reduction procedure can be derived from solutions of the heat conduction equation, together with appropriate initial and boundary conditions corresponding to the thermal flash test. In the case in which the heat flux in the sample is one dimensional, the heat conduction equation is

$$\frac{\partial T}{\partial t} = \alpha \frac{\partial^2 T}{\partial x^2} \quad (0 \leq x \leq L, t > 0) \quad (1)$$

where t is time, α is the thermal diffusivity, x is the space coordinate, L is the sample thickness, and $T = T(x, t)$ is the temperature at the space-time point (x, t) . In the ideal thermal flash experiment, the initial and boundary conditions are

$$T(x, 0) = 0 \quad (2)$$

$$\left. \frac{\partial T}{\partial x} \right|_{x=0} = -\frac{Q}{k} \phi(t) - \frac{h}{k} T(0, t) \quad (3)$$

$$\left. \frac{\partial T}{\partial x} \right|_{x=L} = -\frac{h}{k} T(L, t) \quad (4)$$

where k is the thermal conductivity of the sample, Q is the amount of heat absorbed through unit area of the sample face, h is the heat transfer coefficient and $\phi(t)$ is the flash pulse shape function.

By neglecting the heat loss effect ($h = 0$) and assuming instantaneous pulse heating,

$$\phi(t) = \delta(t) \quad (5)$$

where $\delta(t)$ is the dirac delta function [16], the rear surface temperature of the sample is given by the solution at $x = L$

$$T(t) = T_m \left[1 + 2 \sum_{m=1}^{\infty} (-1)^m \exp\left(-\frac{n^2 \pi^2 \alpha t}{L^2}\right) \right] \quad (6)$$

where

$$T_m = \frac{Q}{\rho c L} \quad (7)$$

is the steady state temperature in the sample after the pulse, ρ is the density, and c is the heat capacity of the sample material. This is the analysis provided by Parker et al. [1].

As an alternative method of solution of the heat transfer equation the rear-face temperature rise can be written using the Laplace transform method [17]

$$T(t) = T_m \frac{2L}{\sqrt{\pi \alpha t}} \sum_{m=0}^{\infty} \exp\left[-\frac{(2n+1)^2 L^2}{4 \alpha t}\right] \quad (8)$$

This series has very good convergence at early times (for small values of t). It is thus complementary to the solution (6) that converges most rapidly at large values of t . In Section 4 we will use the analytical solutions to illustrate the accuracy of our numerical solution and its convergence properties.

3. Numerical method

In the numerical model, time is divided into discrete steps Δt and the thermal flash test specimen is subdivided into N volume elements of thickness Δx along the x axis—the heat flow direction. Using Eq. (1), the temperature $T(x, t)$ is integrated forward in time using the following explicit finite-difference algorithm at the interior points of a uniform grid:

$$\frac{T(x, t + \Delta t) - T(x, t)}{\Delta t} = \alpha \frac{T(x + \Delta x, t) - 2T(x, t) + T(x - \Delta x, t)}{\Delta x^2} \quad (9)$$

At the boundaries Eq. (9) is applied and the $T(-\Delta x, t)$ and $T(L + \Delta x, t)$ that appear are eliminated by using the boundary conditions Eqs. (3) and (4) in the forms,

$$\frac{T(\Delta x, t) - T(-\Delta x, t)}{2\Delta x} = -\frac{Q}{k} \phi(t) - \frac{h}{k} T(0, t) \quad (10)$$

$$\frac{T(L + \Delta x, t) - T(L - \Delta x, t)}{2\Delta x} = -\frac{h}{k} T(L, t) \quad (11)$$

As a result of numerical stability the time step Δt and the grid size Δx are related by Von Neuman relationship [18]:

$$\Delta t \leq \frac{\Delta x^2}{2\alpha} \quad (12)$$

The method is simple to implement in the sense that it is an explicit scheme and advances the solution in time without solving a large systems of equations as is necessary in the implicit method. In demanding situations, extending the method into an implicit scheme and higher order accuracy method can be expected to be straightforward [18,19].

4. Numerical solution and convergence study

In this section we test our numerical method by comparing its solution with the analytical method for the thermal flash test of a homogeneous material. By refining the grid, we will show that the numerical solution converges to the analytical one with negligible truncation errors. For this comparison we consider the situation of no heat loss and instantaneous pulse heating, for which the analytical solution can be given by Eq. (6) or equivalently, Eq. (8). Typical results are shown in Fig. 1, where the simulated temperature were calculated from Eqs. (9)–(11). The input parameters used for the comparison were $\alpha = 0.01 \text{ cm}^2/\text{s}$, $L = 0.1 \text{ cm}$, $T_m = 2 \text{ }^\circ\text{C}$. The number of volume elements $N = 2, 5, 10$ was used respectively in the numerical solution. The analytical solution was calculated by using both Eq. (8) for small values of t and Eq. (6) for larger values of t .

From the figures we can see by using more and more refined grid $N = 2, 5, 10$, the numerical solution converged to the analytical one. For $N = 10$, there is little difference between them, but for greater confidence, we will use $N = 20$ in all the later runs.

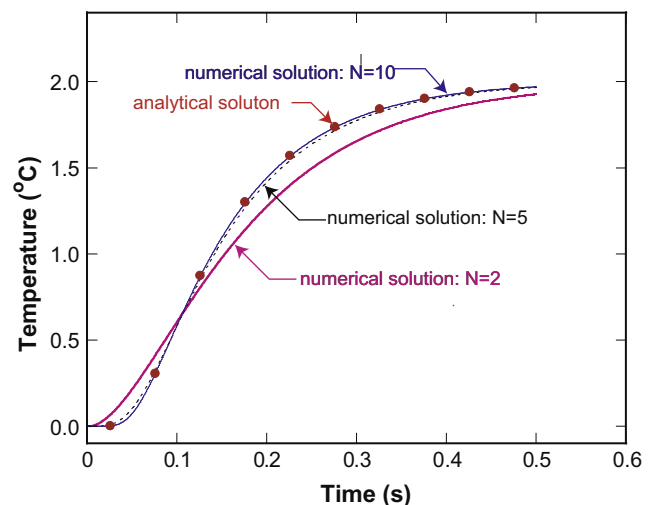


Fig. 1. Comparison of numerical solution to analytical solution in normalized thermograms. Input data $\alpha = 0.1 \text{ cm}^2/\text{s}$, $L = 0.1 \text{ cm}$, $T_m = 2 \text{ }^\circ\text{C}$. N is the number of volume elements used in the numerical solution.

Although the test is only for the ideal case of no heat loss and instantaneous pulse heating, the method is more general and will apply to more complicated situations with heat losses or/and with finite pulse heating effect.

5. Parameter estimation

The parameter estimation approach to data reduction involves determination of parameters of interest through fitting of a calculated model to experimentally obtained data. The fitting is performed by minimizing the mean square error between the measured temperature versus time data and that predicted from numerical solutions. The parameters of interest serve as the variables for the curve fitting process. A comprehensive treatment of the parameter estimation method is presented by Beck and Arnold [20].

In the thermal flash experiment, the data points are $(t_1, T_1), (t_2, T_2), \dots, (t_n, T_n)$, where t is time, the independent variable, and T is the detected back face temperature, the dependent variable. The fitting curve $f(t)$ has the deviation d from each data point, i.e., $d_1 = T_1 - f(t_1), d_2 = T_2 - f(t_2), \dots, d_n = T_n - f(t_n)$. According to the method of least squares, the best fitting curve has the property that:

$$\begin{aligned} \Pi &= d_1^2 + d_2^2 + \dots + d_n^2 = \sum_{i=1}^n d_i^2 = \sum_{i=1}^n [T_i - f(t_i)]^2 \\ &= \text{minimum} \end{aligned} \quad (13)$$

The advantages of this method are that [14],

- It can reduce the effect of noise distortions to the transient signal, and it becomes especially useful, when noisy data prevent simple application of more standard techniques.
- By comparing the experimental data and the calculated curve, poor quality data and irregularities can be identified. Thus, only good quality experimental data are used, and therefore, less variability between data from successive experiments can be obtained.

5.1. Grouping the parameters

In the thermal flash method we are interested in determining the thermal diffusivity, but as indicated in Eqs. (1)–(4), there are also some other parameters Q, k, h that are either unknown or poorly known. Not all of them can be determined by the parameter estimation process but specific groups of parameters can be identified [20], in this case, $Q/k, h/k$. To make it more intuitive, we substitute the parameters as follows:

$$\frac{Q}{k} = \frac{T_m \rho c L}{k} = \frac{T_m L}{\alpha} \quad (Q = T_m \rho c L) \quad (14)$$

$$\frac{h}{k} = \frac{hL}{k} \cdot \frac{1}{L} = \frac{Bi}{L} \quad \left(Bi = \frac{hL}{k} \right) \quad (15)$$

where Bi is the Biot number, the nondimensional parameter for characterizing the heat loss [21] and T_m is the steady state temperature of the sample after the pulse which can characterize the laser pulse energy absorbed by the sample. The sample thickness L is easily measured leaving the other unknown parameters: α, Bi , and T_m to be determined by the parameter estimation process.

5.2. Sensitivity coefficients

As part of the procedure of obtaining a nonlinear least-squares curve fit to the experimental data, the sensitivity coefficients, S_i , [20], can be determined,

$$S_i = P_i \frac{\partial \tilde{T}}{\partial P_i} \quad (16)$$

where \tilde{T} is the normalized temperature rise, $\tilde{T} = T/T_m$, and P_i are the curve fit parameters. S_i may be thought of as the fractional change in temperature produced by a unit fractional change in P_i . The value of these sensitivity coefficients is that they indicate the relative importance of the fit parameters. In general the sensitivity coefficients are desired to be large, especially the one associated with the thermal diffusivity. What is more, the sensitivity coefficients can help identify calculational regimes where the parameters are most sensitive and hence the optimal region to perform the fitting. These sensitivity coefficients for a simulated run from the numerical solution are shown in Fig. 2. The input parameters were $\alpha = 0.01 \text{ cm}^2/\text{s}$, $L = 0.1 \text{ cm}$, $T_m = 2 \text{ }^\circ\text{C}$, the same as in Fig. 1, together with $Bi = 0.1$. The figure reveals the following information:

- The magnitude of the sensitivity coefficient for diffusivity is high and is most sensitive around the half-time – the time in which the rear-face temperature rise reaches one half of its maximum value [1].
- The solution is not very sensitive to the heat loss parameter Bi but is sensitive to the temperature rise T_m or absorbed energy Q , especially at later times when the temperature is close to the maximum.

5.3. Implementation on simulated data

As a further test, we compare the calculation with a variety of simulated data. Typical results are shown in Figs. 3–5. Fig. 3 shows simulated input data calculated from Eqs. (9)–(11) with the addition of Gaussian noise and assuming instantaneous pulse heating Eq. (5). The input parameters were again $\alpha = 0.01 \text{ cm}^2/\text{s}$, $L = 0.1 \text{ cm}$, $T_m = 2 \text{ }^\circ\text{C}$, $Bi = 0.1$, where standard deviation of noise is 5% of T_m . In the parameter estimation process, the initial values of α, Bi and T_s are given, and the iteration is carried out until the corresponding convergence condition is met. Here the residuals of the parameters are less than 0.1%. The Matlab [22] function “nlinfit” has been adopted to complete the estimation process.

Fig. 4 shows the calculated fitted temperature vs time profile by using the whole range of data from input. We note that the fitting process is quite successful and all the three parameters α, Bi and T_s

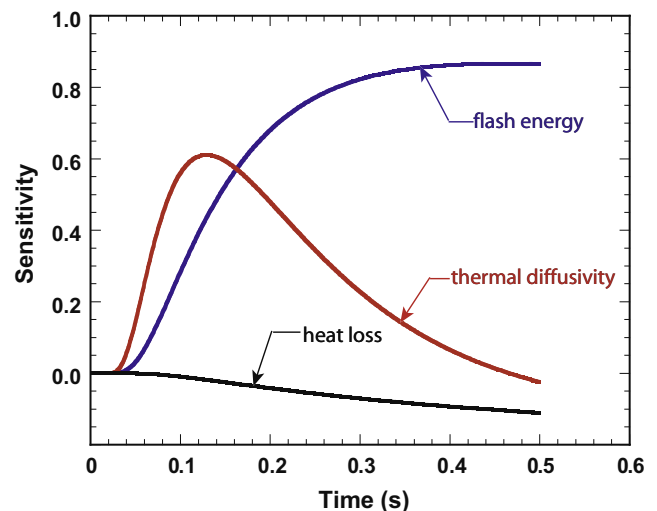


Fig. 2. Sensitivity coefficients for simulated run with $\alpha = 0.01 \text{ cm}^2/\text{s}$, $L = 0.1 \text{ cm}$, $T_m = 2 \text{ }^\circ\text{C}$, $Bi = 0.1$.

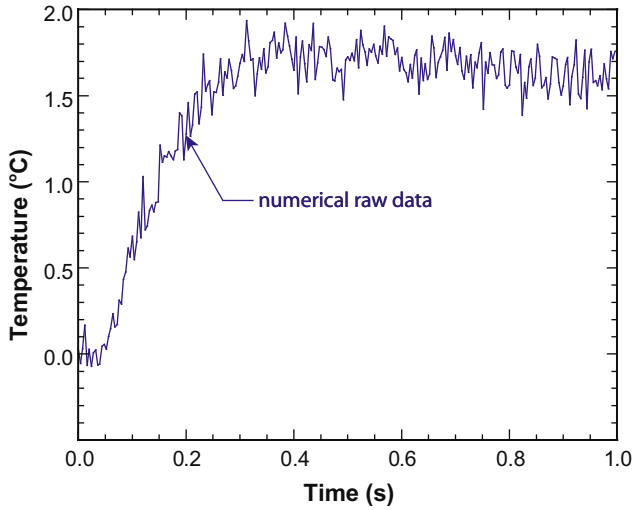


Fig. 3. Simulated data with Gaussian noise. Input data to run was $\alpha = 0.01 \text{ cm}^2/\text{s}$, $L = 0.1 \text{ cm}$, $T_m = 2 \text{ }^\circ\text{C}$, $Bi = 0.1$. The standard deviation of noise is 5% of T_m .

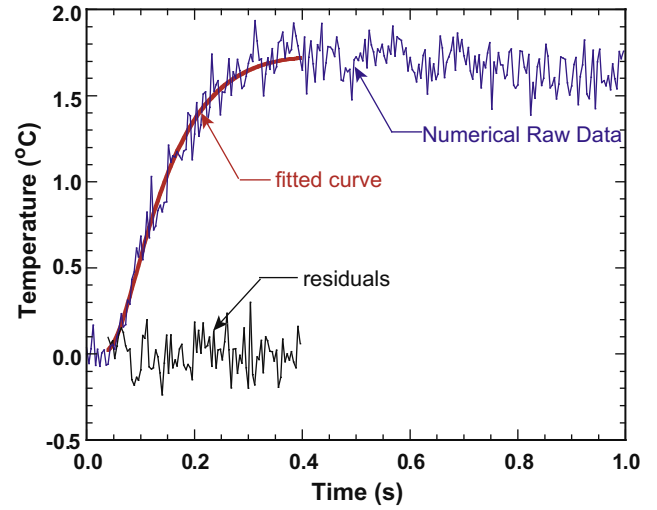


Fig. 5. Curve fit by using the data range from $t = 0.04$ to $t = 0.4$. Calculated results were $\alpha = 0.10017 \text{ cm}^2/\text{s}$, $T_m = 1.9484 \text{ }^\circ\text{C}$, $Bi = 0.0626$.

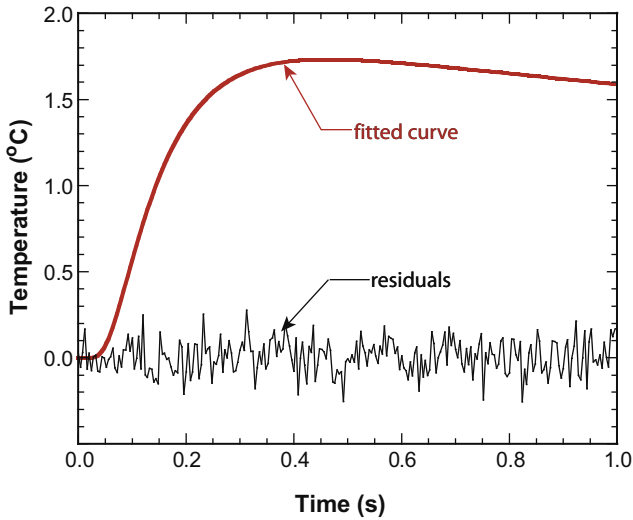


Fig. 4. Curve fit by using the whole range of data shown in Fig. 3. Calculated results were $\alpha = 0.09957 \text{ cm}^2/\text{s}$, $T_m = 2.0019 \text{ }^\circ\text{C}$, $Bi = 0.0991$.

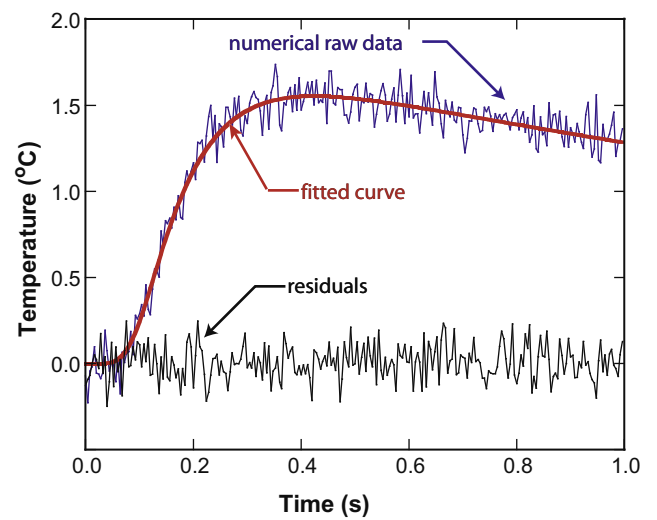


Fig. 6. Curve fit by “method I”. Calculated results were $\alpha = 0.9972 \text{ cm}^2/\text{s}$, $T_m = 1.9996 \text{ }^\circ\text{C}$, $Bi = 0.2007$.

are determined within 1%. Next we limited the data range of fitting from $t = 0.04$ to $t = 0.4$, the time over which the thermal diffusivity has the highest sensitivity values, but T_m and Bi are not as sensitive as shown in Fig. 2. The results are shown in Fig. 5. In agreement with the sensitivity coefficients predictions, the accuracy of both T_m and Bi dropped substantially, especially Bi has nearly 40% in error, while the determination of the diffusivity is still accurate, $\sim 1\%$. As suggested by this simulated example, in an actual application of the data reduction scheme, we may pick the data range of fitting more efficiently, rather than simply fitting the whole range of data.

5.4. Finite pulse-width correction

Sometimes it is necessary to take into account the correction due to the finite duration and shape of the heat pulse, for example, when thin samples of high thermal diffusivity are tested or a broad band radiative heating source is used instead of a pulsed laser. Various corrections have been described in the literature to take into account the shape of the heat pulse, [23,3,5,24,25]. In each case, the heat pulse shape was known. To include the finite pulse-width

correction into our data reduction method, we considered two methods:

- (I) If we know the pulse shape function $\phi(t)$, we can use it in Eq. (10). Then, the parameter estimation process can be applied as before. We will refer to this as “method I”.
- (II) If we do not know the pulse shape function, or we can not measure it accurately, we use the procedure of Azumi and Takahashi [25]. However, instead of shifting the time origin explicitly as they do, we will simply add a new unknown t_g to our parameter estimation task. t_g should be regarded as an adjustment for the infinite pulse-width with respect to the “effective” irradiation time. We will refer to this as “method II”.

Fig. 6 shows simulated raw data together with the fitted curve obtained by using the above mentioned “method I”. The input parameters were $\alpha = 0.01 \text{ cm}^2/\text{s}$, $L = 0.1 \text{ cm}$, $T_m = 2 \text{ }^\circ\text{C}$, $Bi = 0.2$ and a square wave pulse of width $\tau = 0.06$, almost half of the half-time, $t_{1/2} \sim 0.1388$ [1]. Again, the fitting process was quite successful

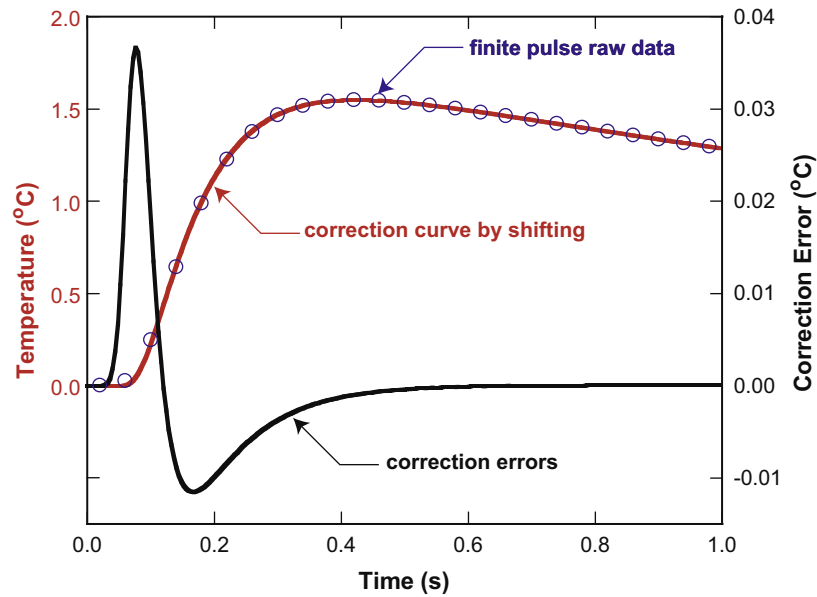


Fig. 7. Finite pulse-width correction [25]. There is no noise disturbance in the simulated raw data, but with finite pulse-width effect. The error magnitude should read from the right y axis.

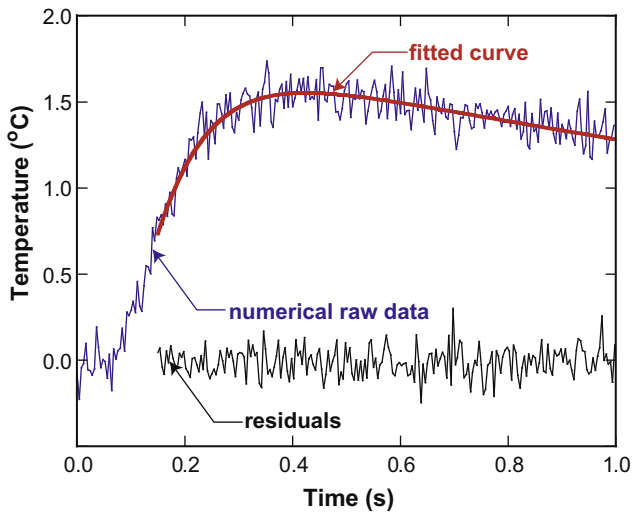


Fig. 8. Curve fit by “method II”. Calculated results were $\alpha = 0.9929 \text{ cm}^2/\text{s}$, $T_m = 2.0077 \text{ }^\circ\text{C}$, $Bi = 0.9856$, $t_g = 0.0304$.

since all the three parameters are determined within 1%. For “method II” we have to pick the data range to fit the curve, since the time origin is shifted. Fig. 7 shows the error caused by the correction of simply shifting the time axis as Azumi and Takahashi [25] have done, where there is no noise disturbance in the raw data. As expected, there is large error near the origin, but after twice the pulse-width τ , it rapidly decays. So we want to pick the data range far from the origin, but determination of the thermal diffusivity requires that the range be within the high sensitivity range. There are no unique rules, so here we arbitrarily pick three times the pulse-width τ as a starting point. Fig. 8 shows the fitted curve. Though the results are not as accurate as using “method I”, the thermal diffusivity was determined $\sim 1\%$. Also we notice that the t_g is very close to value calculated by using the center of gravity of the pulse shape, a criterion introduced in reference [25]. An advantage of this second method is that we do not have to know the pulse shape. This is a significant advantage since the heat

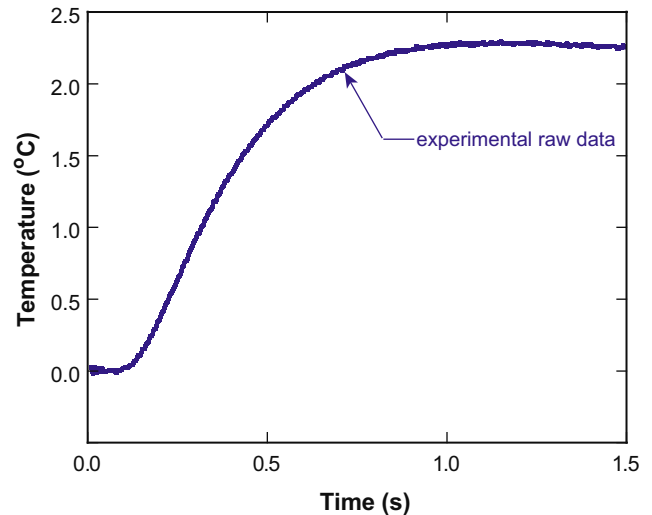


Fig. 9. Temperature response curve from experimental measurement.

pulse may not be simply characterizable or it may change from test to test as well as from day to day.

6. Implementation on experimental data

In order to demonstrate the utility of this data reduction method, we present results obtained in determining the thermal diffusivity of a number of materials ranging from an opaque ceramic sample of pyroceram, a materials often used as a reference calibration sample, which has a low thermal diffusivity to copper, a high thermal diffusivity material.

6.1. Experimental apparatus and measurement method

The measurements were conducted on a Flashline 3000 instrument from Anter Corporation. This instrument uses a xenon flash lamp under computer control to impart a brief but controlled

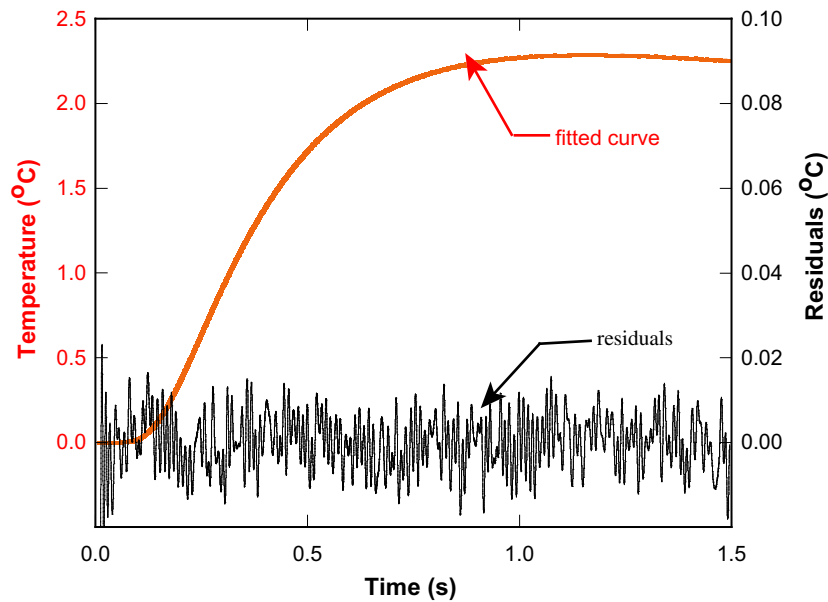


Fig. 10. Curve fit by “method II”. Calculated results were $\alpha = 0.0159 \text{ cm}^2/\text{s}$, $T_m = 2.7993 \text{ }^\circ\text{C}$, $Bi = 0.1512$, $t_g = 0.0018$.

amount of energy to the sample. The light travels through a quartz light pipe, which helps to ensure that the entire front side surface of the sample is evenly heated, to illuminate the test sample. A similar light pipe at the back side of the sample conducts the radiation to a liquid nitrogen cooled infrared detector. The detector measures the sample temperature and outputs a voltage to the system electronics, which are controlled by the analysis software. The software also controls the timing of the flash pulse, giving the thermal history of the sample from a few seconds before the pulse to several seconds after the pulse. From the voltage as a function of time, the built-in software can calculate several thermal diffusivity values using the corrections described in Refs. [2,26,7,8].

The specimen thickness at three different positions was measured using a micrometer and the average value was adopted in the diffusivity calculation. The thermal flash measurements were made with the sample held at a temperature of around $100 \text{ }^\circ\text{C}$. The average pulse width is $\sim 300 \mu\text{s}$ to $600 \mu\text{s}$. We used “method II” to correct the finite pulse effect, since we do not know the shape of the pulse function. Generally it is hard to determine the actual shape of the heat pulse delivered by the flash lamp because of its multi-wavelength spectral nature.

6.2. Experimental results

Fig. 9 shows the temperature rise curve, the experimental thermogram, measured for the Pyroceram sample. The raw data are detector output voltage which can be changed into temperature rise. Also, the data has been smoothed by a high frequency noise filter in the system, but there is still noticeable low frequency noise which is difficult to remove [9]. In accord with the above mentioned sensitivity analysis, we have taken into account the experimental points which lie in the the rising part of the temperature vs time curve. Fig. 10 shows the calculated fitted curve with the residuals. The magnitude of the residuals should be read from the right y axis. From the random distribution shape of the residuals, we can see the fitted curve agrees well with the the experimental curve. A comparison of our results with the results determined by other methods implemented in the Anter software from the same measurement data is given in Table 1 and shows that the present method of data reduction is comparable in accuracy with other special methods [1,2,6,26,7,8] including ones using laser pulse heating as

Table 1

Diffusivity, in cm^2/s , determined using different analysis method.

Method		Pyro	SC-180	SS	Cu
Parker et al. [1]		0.0174	0.0269	0.0442	1.1464
Cowan [2]	5 $t_{1/2}$	0.0159	0.0240	0.0404	1.0256
	10 $t_{1/2}$	0.0160	0.0251	0.0414	1.1327
Clark and Taylor [26]	$t_{0.7}/t_{0.3}$	0.0159	0.0254	0.0425	1.0878
	$t_{0.8}/t_{0.4}$	0.0160	0.0260	0.0409	1.2169
	$t_{0.8}/t_{0.2}$	0.0158	0.0250	0.0413	1.1682
Degiovanni [7]	2/3	0.0152	0.0245	0.0423	1.5176
	1/2	0.0157	0.0253	0.0434	1.2310
	1/3	0.0161	0.0261	0.0412	1.2641
Koski [8]		0.0160	0.0252	0.0415	1.1451
Present work		0.0159	0.0246	0.0425	1.2056

The measurement precision is probably no better than the third significant number. “Pyro” is Pyroceram, a tradename, provided by Anter as a calibration material; “SC-180” is a single crystal super-alloy material used for TBC substrate in industry; “SS” is a stainless steel material provided by UCSB machine shop; “Cu” is a copper material also provided by Anter as a calibration material.

distinct from the flash lamp sources. Calculations and comparisons for all materials are also included in the table.

7. Concluding remarks

This paper presents a new data reduction method for determining thermal diffusivity from thermal flash experiments. It is based on numerical solutions of the heat conduction equation and uses a nonlinear parameter estimation technique. Experimental temperature vs time data are first recorded, then the calculated curve from numerical simulation is fitted to the experimental temperature-time curve. The method was first tested on sets of simulated data and then on sets of experimental thermal flash data.

Although the results show that the accuracy of our procedure is comparable with that of other methods for determining thermal diffusivity from thermal flash measurements for simple materials under well defined conditions, the real advantage of the method is that radiation heat loss and finite pulse-width effects can be readily corrected. More importantly, the effect of a finite pulse-width can be eliminated without knowing the precise shape and duration of the heat pulses. Also following the spirit of current work, it is expected to be relatively straightforward to extend this

method for two or multi-layer materials, which have very complicated analytical solutions.

References

- [1] W.J. Parker, R.J. Jenkins, C.P. Butler, G.L. Abbot, *J. Appl. Phys.* 32 (9) (1961) 1679.
- [2] R.D. Cowan, *J. Appl. Phys.* 34 (4) (1963) 926.
- [3] R.E. Taylor, L.M. Clark III, *High Temp. High Press.* 6 (1974) 65.
- [4] J.A. Cape, G.W. Lehman, *J. Appl. Phys.* 34 (7) (1963) 1909.
- [5] K.B. Larson, K. Koyama, *J. Appl. Phys.* 38 (2) (1966) 465.
- [6] R.C. Heckman, *J. Appl. Phys.* 44 (4) (1973) 1455.
- [7] A. Degiovanni, *Rev. Gen. Therm.* 185 (1977) 417.
- [8] J.A. Koski, *Proceedings of the 8th Symposium on Thermophysical Properties*, vol. 2, The American Society of Mechanical Engineers, New York, 1981. p. 94.
- [9] L. Pawlowski, P. Fauchais, C. Martin, *Rev. Phys. Appl.* 20 (1985) 1.
- [10] L. Pawlowski, P. Fauchais, *Rev. Phys. Appl.* 21 (1986) 83.
- [11] J. Gembarovič, L. Vozár, V. Majerník, *Int. J. Heat Mass Transfer* 33 (7) (1990) 1563.
- [12] M. Raynaud, J.V. Beck, R. Shoemaker, R. Taylor, *Therm. Conduct.* 20 (1989) 305.
- [13] J.V. Beck, R. Dinwiddie, *Therm. Conduct.* 23 (1996) 107.
- [14] A. Cezairliyan, T. Baba, R. Taylor, *Therm. Conduct.* 15 (1994) 317.
- [15] J.V. Beck, *Inverse Problems in Engineering/Theory and Practice*, ASME, New York, 1998. p. 531.
- [16] J. Gemvarovič, R.E. Taylor, *In. J. Thermophys.* 14 (1993) 297.
- [17] L. Vozár, W. Hohenauer, *High. Temp. High. Press.* 35 (2003/2004) 253.
- [18] J.H. Ferziger, M. Perić, *Computational Methods for Fluid Dynamics*, Springer, New York, 2002.
- [19] C.A.J. Fletcher, *Computational Techniques for Fluid Dynamics*, Springer, New York, 1987.
- [20] R.C. Beck, K.J. Arnold, *Parameter Estimation in Engineering and Science*, John Wiley and Sons, New York, 1977.
- [21] William M. Deen, *Analysis of Transport Phenomena*, Oxford university press, New York, 1998.
- [22] Matlab – The Language of Technical Computing. <<http://www.mathworks.com/products/matlab>>.
- [23] D.A. Watt, *Brit. J. Appl. Phys.* 17 (1966) 231.
- [24] R.E. Taylor, J.A. Cape, *Appl. Phys. Lett.* 5 (10) (1964) 212.
- [25] T. Azumi, Y. Takahashi, *Rev. Sci. Instrum.* 52 (1981) 1411.
- [26] L.M. Clark III, R.E. Taylor, *J. Appl. Phys.* 46 (2) (1975) 714.